EULER-BERNOULLI THEORY ACCURATELY PREDICTS ATOMIC FORCE MICROSCOPE CANTILEVER SHAPE DURING NON-EQUILIBRIUM SNAP-TO-CONTACT MOTION

Steven J. Eppell,[1,§] David Friedenberg,[2] Oliver Payton,[3] Loren Picco,[4] Fredy R. Zypman,[2,§]

[1]Biomedical Engineering Dept., Case Western Reserve University, 10900 Euclid Ave., Cleveland, Ohio, 44122 USA
sje@case.edu

[2]Physics Dept., Yeshiva University, 2495 Amsterdam Ave., Manhattan, New York, 10033 USA
zypman@yu.edu, dfriede1@mail.yu.edu

[3]Interface Analysis Centre, H. H. Wills Physics Laboratory, University of Bristol, Bristol, UK
op4664@bris.ac.uk

[4]Physics Dept., Virginia Commonwealth University, Richmond, VA, 23284 USA
lpicco@vcu.edu

§Corresponding authors sje@case.edu, zypman@yu.edu

ABSTRACT

We prove that the Euler-Bernoulli elastic beam theory can be reliably used to describe the dynamics of an atomic force microscope cantilever during the far from equilibrium snap-to-contact event. In conventional atomic force microscope operation, force-separation curves are obtained by post-processing voltage versus time traces produced by measuring one point on the cantilever close to the hanging end. In this article, we assess the validity of the Euler-Bernoulli equation during the snap-to-contact event. The assessment is based on a direct comparison between experiment and theory. The experiment uses Doppler vibrometry to measure displacement versus time for many points along the long axis of the cantilever. The theoretical algorithm is based on a solution of the Euler-Bernoulli equation to obtain the full shape of the cantilever as a function of time. The algorithm uses as boundary conditions, experimentally obtained information only near the hanging end of the cantilever. The solution is obtained in a manner that takes into account non-equilibrium motion. Within experimental error, the theory agrees with experiment indicating that the Euler-Bernoulli theory is appropriate to predict the cantilever kinematics during snap-to-contact. Since forces on the tip can be obtained from the instantaneous shape of the cantilever, this work should allow for computation of tip-sample forces during the snap-to-contact event from a conventional force-distance measured input.

Key Words: AFM, atomic force microscopy, far from equilibrium AFM cantilever, force distance curve

INTRODUCTION

The central hypothesis of this paper is that the Euler-Bernoulli equation provides a valid model by which the kinematics of an AFM cantilever can be obtained during the far-from-equilibrium snap-to-contact event. This event is often purposely avoided to stay within the regime in which harmonic analysis can be performed. However, the snap-to-contact presents a unique opportunity to test samples at closest approach. It allows for optimal sensitivity to rapidly changing surface forces, allows for optimal lateral resolution because the situation can be analyzed at arbitrarily small tip-sample separation, and provides a method for obtaining these results with a simple experimental setup that requires no lock-in amplifiers. Motivated by these observations, we sought to determine if a conventional AFM that provides cantilever displacement measures only at the hanging end, can be used in conjunction with the Euler-Bernoulli equation to obtain the full cantilever kinematics. Since forces on the tip can be obtained from the instantaneous shape of the cantilever,[1] this work should allow for computation of tip-sample forces during the snap-to-contact event from a conventional force-distance measured input.

Atomic force microscopy is capable of generating topographical and surface spectroscopic information even at length scales below a nanometer. To obtain this information reliably and quantitatively, it is necessary for the user to know what forces the cantilever experiences at each instant of operation. Thus, the mathematical prediction of the kinematics of the cantilever sensor plays a central role in defining the output accuracy of the force reconstruction algorithm in atomic force microscopy. To date, this description is well tested for quasi-static operation and for operation where the cantilever is driven in one or more of its normal modes. In this article, we study the validity of the assumption that the cantilever's kinematics can be obtained from the Euler-Bernoulli equation [2-4] even under the specific conditions of non-equilibrium motion and non-linear external forces. These common circumstances exist during the snap-to-contact event, when the atomic force microscope tip experiences the last few nanometers of travel before impacting the surface.

While the non-equilibrium motion mentioned above is not present in multifrequency operation,[5, 6] the newer commercially available techniques involving off-resonance motion of the lever as accomplished with peak force mode and fast force mapping do contain non-equilibrium motion[7]. These methods take the lever through a single stroke similar to the slow force-separation curve dealt with in the present paper.

In the past three decades, atomic force microscopy[8] has produced images of soft and hard matter surfaces with submicron, even nanometer resolution [9-18]. Nevertheless, considering its recent centrality in the imaging of materials surfaces and the vast technical improvements regarding data collection speed and resolution, [5, 19] the technique is not yet completely quantitative. This is due to a large extent both to the lack of full information of the interaction forces between the sample and the tip, and to an unavoidable mismatch between the mathematically modeled cantilever and the real one.

Since the inception of atomic force microscopy, imaging has been based on monitoring variations of experimental parameters as the cantilever/tip sensor moves from one pixel to the next. In the conventional experimental implementation of the image reconstruction, an optic lever system is used to measure the position of the tip or, more accurately, the slope of the cantilever at the tip's position. A photodetector output voltage is rapidly recorded at each pixel while the tip moves up and down as a consequence of topographical and chemical variations on

the surface. Thus, by looking at all pixels within the field of view, a surface image can be rendered using some function of the photodetector voltage as the contrast quantity.

A fundamental question presents itself naturally; what is the physical content of the voltage in regards to the surface under study? Answering this question is tantamount to learning which tip-sample interaction forces are at play in producing a motion of the cantilever, which ultimately generates the observed voltage. To build the voltage-to-force connection, it is necessary to have a reliable mathematical model that produces the kinematics of the cantilever. This model is then used to answer several questions. How does the tip sensor move under external forces? How does that induced motion effect a photodetector voltage? How does one solve the inverse problem whereby the experimental voltage, conventionally known only from the motion at one location on the cantilever, is used to reconstruct the motion of the cantilever at all points and for all times, and in due course, the sought forces acting on it?

Usually, a minimalistic connection is made between forces and voltages where, via simplifying approximations, the voltage is proportional to the force at every instant. The corresponding underlying assumptions, that the cantilever's deflection at its free end is proportional to the slope there, and a one-degree-of-freedom-cantilever, are too stringent for quantitative force analysis when the system is far from equilibrium.[20] More accurate approaches include treating the cantilever as a simple harmonic oscillator[21] and even more realistically, as a true extended beam that can support spatial and temporal vibrations.[20] The Euler-Bernoulli beam theory is particularly relevant to a wide range of atomic force microscopy applications because the slim cantilever's vibrations are dominated by its flexural motions. In effect, the Euler-Bernoulli equation provides a rigorous connection between the complete shape of the cantilever and the force history required to produce that shape. Thus, if the shape of the cantilever is measured experimentally and this agrees with the shape predicted by the Euler-Bernoulli equation, this is synonymous with stating that the forces experienced by the system can be accurately recovered using the Euler-Bernoulli equation. This is the central thesis driving the work we present. The work is based on an experimental design whereby the cantilever's position-vs-time curves are measured at multiple locations, not just at one point near the hanging end.

Several previous studies have looked at the problem of validating the accuracy of the Euler-Bernoulli theory in predicting the behavior of real atomic force microscope cantilevers. Some of this work is reviewed below. This literature provides results that are both interesting and useful to the atomic force microscopy community. However, none of the extant studies simultaneously and directly compares experiment to theory for the cantilever under non-equilibrium conditions.

Payam and Fathipour[22] performed a theoretical analysis of the Euler-Bernoulli equation by means of variational analysis with the goal to incorporate practical aspects of the microscope such as tip mass and cantilever geometry. Gates and Pratt[23] used Doppler vibrometry in conjunction with Euler-Bernoulli analysis to measure the cantilever's spring constant with high accuracy. This analysis did not address either transient behavior nor the full shape of the cantilever. Payton et al.[24] tackled the problem of fast imaging whereby an unknown varying force acts on the tip due to surface topography variations. While they did measure the shape of the cantilever as a function of time, the study was restricted to eigenmodes of the combined cantilever/sample system; amplitudes of the cantilever's vibration were collected at different locations at a single frequency for times long relative to the snap-to-contact event to increase reliability. This method cannot be used in our case because the snap-to-contact

determines naturally and suddenly what happens to the deflection of the cantilever. Zhou, Fu and Li [25] used the Euler-Bernoulli theory to extract mechanical properties of composite materials. While they did not deal with the full shape of the cantilever, they did compare Euler-Bernoulli with finite element analysis and validated the appropriateness of Euler-Bernoulli to within three percent under dynamic equilibrium conditions. Laurent, Steinberger and Bellon [26] considered a cantilever with a spherical bead at its end. They compared the normal mode shapes of Euler-Bernoulli theory with experimentally measured ones and got agreement to within ten percent for the first four modes. While they were able to measure the shape of the cantilever at multiple points versus time, they did it for normal modes and not for the general transient case. Payam[27] studied the shift in frequencies due to the presence of an ambient liquid and used the Euler-Bernoulli equation to analyze the signal but did not consider the shape of the cantilever or transient behavior. Villanueva et al.[28] were interested in the length limits of the Euler-Bernoulli equation. They found that 20 μm long levers, corresponding in their case to a cantilever length:width aspect ratio of about five, are short enough to make the theory deviate from experiments. Zhou, Wen and Li [29] presented a theoretical study of short cantilevers and showed how to correct the Euler-Bernoulli equation via the Timoshenko theory. Their paper did not present experimental comparison nor did it consider the shape of the cantilever or transient behavior. Wagner and Killgore[30] studied the resonant motion of a cantilever under the effect of lumped or distributed forces. No transient or experimental measurements were considered.

In general, the difficulty in providing a definite account of the agreement between experiment and theory resides in both. On the one hand, typical atomic force microscopes are not set up to measure rapid cantilever deflections at multiple points along the lever. Thus, the full shape of the lever necessary to determine unambiguously the forces acting on it is not available. On the other hand, the theories rely on reasonable assumptions fit to the problem of interest. Thus, for example, one may be interested in cantilever free boundary conditions at the hanging end for spring constant calibration, or harmonic excitations at the base for multi frequency studies. All articles in this field use the Euler-Bernoulli equation with adaptations pertinent to the problem at hand.

In this context, the present paper presents new data and analysis useful in the unsolved problem of understanding the connection between theory and experiment during the snap-to-contact event. We previously showed that the classic concave up surface potential vs separation could be extracted from this motion in air [3] and in liquid [31]. These earlier papers utilized Tikhonov regularization to solve the inverse problem imposed by only having experimental measurement of the end of the lever while solution of the problem requires knowledge of the full lever shape. This is an ill-posed inversion for cases involving fast transients, like in the snap-to-contact. We inverted the Euler-Bernoulli equation in the cantilever's shape space spanned by the normal modes under conditions of an unloaded tip. This was an intrinsically limited method since, during the snap-to-contact, the tip load quickly increases thus violating the assumption of an unloaded tip used to create the basis set. More recently, we developed what should be a more robust method for converting the voltage-vs-time trace produced by the vertical motion of the tip measured at a single cantilever location into forces, the Causal Time Domain Analysis (CTDA).[32] CTDA relies on explicit consideration of the measured nonlinear voltage-time data as a boundary condition to the Euler-Bernoulli equation. When we compared Tikhonov regularization to CTDA, we found that the two approaches did not produce the same force-separation curves.[2] An obvious next step would be to use some known surface force to determine which theory performed better. However, there is currently no well-accepted standard

for creating a surface force that is known within a few nanometers of tip/surface contact. Thus, we decided to test CTDA against experimentally measured cantilever shapes. The choice is based on the fact that CTDA, unlike regularization, is free of tuning parameters. That is what we present in the current article, which is organized as follows. In the Methods section, we explain how conventional AFM measurements are performed and give details of our experimental setup. Also, in the Methods section, a brief description of our theory is presented. Then, in the Experimental Results section, we present the position versus time traces at multiple points along the cantilever. In the Comparison of Theory and Experiment section, we show how the theory output, i.e. the full shape of the cantilever at all times, matches with the experiment. In the last section, we present the Conclusions.

METHODS

Conventional Experimental Approach

Standard atomic force microscopes come equipped with a light detection system to measure the motion of the cantilever as shown in Figure 1. A light ray reflected off the cantilever provides a photodetector voltage that is proportional to the slope of the cantilever at the hanging end.

However, and as Figure 1 depicts, the instantaneous value of the slope at one point provides only partial information of the full shape of the cantilever at that instant. Since the full shape is necessary to determine the interaction force between tip and sample but is not typically available experimentally, mathematical modeling is called upon to bridge the gap between what is needed and what experiment provides.

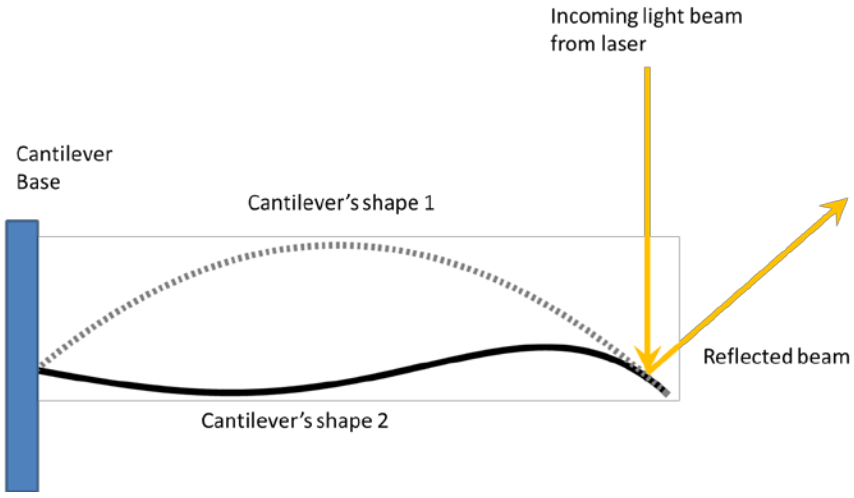

Figure 1. An incoming light ray shown as a vertical line impinges at the hanging end of the cantilever. Here the cantilever is portrayed in two different shapes both having the same z-location and slope at the end of the lever. This will produce the same voltage at the distant photodetector even though different forces are needed to produce the two shapes.

One quantitative approach to make the connection relies on the Euler-Bernoulli equation to predict the motion of the cantilever.[33] In one implementation using this approach[32], the instantaneous slope, proportional to the photodetector voltage, is used as a boundary condition to the Euler-Bernoulli equation. By assuming a straight cantilever as an initial condition to the problem, corresponding to a large tip-sample separation at the beginning of the experiment when

no interaction forces are detectable, the equation can be solved iteratively in time to obtain the full shape of the cantilever at all future times. With this information, the interaction force at all times is finally obtained. Afterwards, by incorporating instantaneous separation data, the sought force-separation curve is obtained parametrically in time.

Experimental Setup and Considerations

The experiment is in the form of displacement versus time measurements for many points along the long axis of the cantilever. By contrast, conventional data collection in atomic force microscopy is at a single point, typically near the hanging end of the cantilever. Laser Doppler vibrometry was used to monitor the motion of multiple points along the length of the cantilever at multiple times during the snap-to-contact. A schematic of the equipment used is shown in Figure 2. The method used was similar to that described in Payton et al.[34] Briefly, a vibrometer (Polytec VIB-A-510) was attached to a cantilever mount at 12.5°. This allowed for the velocity of the cantilever in the direction perpendicular to the lever's surface to be recorded with high bandwidth (up to 20 MHz). The substrate (a piece of freshly cleaved mica) was cycled sinusoidally toward and away from the cantilever tip (Bruker MSNL lever B, 200 μm long rectangular Si_3N_4 cantilever with a spring constant of 0.02 N/m, a thermal tune measured first mode resonance of 14.65 kHz, and a pyramidal tip) using a piezo stage (Npoint model NPXY60Z20) with closed loop capacitance control at 50 Hz with an amplitude of 850±0.1 nm (maximum velocity was therefore 267 μm/s). The data displayed was collected at the point in the motion of the stage with the sample moving towards the cantilever tip at a velocity of 150±7 μm/s. Z-motion monitoring was done along the cantilever every 1 μm while the cantilever underwent multiple snaps-to-contact. To do signal averaging over several snaps at the same point and to create an experimentally determined cantilever shape, it was necessary to

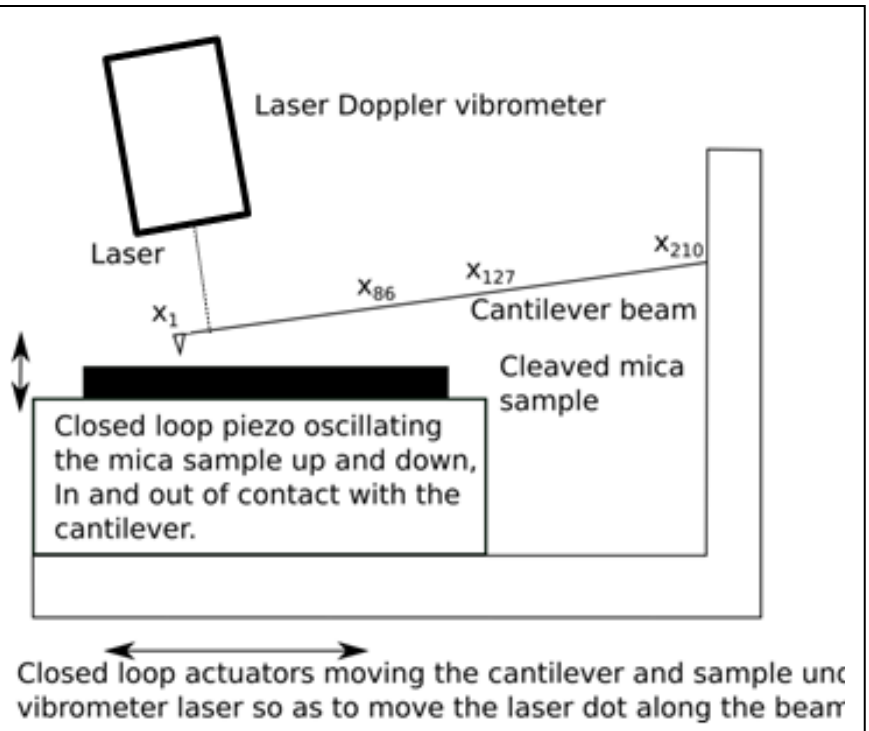

Figure 2: Diagram of the setup used to experimentally measure cantilever deflections during the snap-to-contact. The cantilever is shown with indices along the long axis of the cantilever each separated by 1 um.

shift the individual snaps so they were in-phase with each other. This was done by cross-correlating the data streams over a short time period that spanned the snap-to-contact.

The approach velocity was taken into account when converting the difference in piezo position and cantilever deflection into tip-sample separation. Under the conditions used in our manuscript, the approach velocity was very slow compared to the cantilever velocity due to the snap-to-contact. So, there was unlikely to have been any significant modification in the situation seen by the tip due to the moving sample. The average speed of the cantilever during the snap was about 1600 μm/s. Thus, during the 25 μs of the snap as the tip traversed the 40 nm until contact, the stage moved by 3.8 nm. This was taken into account when producing the force-separation plots shown in the manuscript. While there was a slight drift present in the system causing the tip to snap to contact with the sample at a slightly different point in the periodic motion of the sample, this produced a sub-nanometer uncertainty in the tip-sample distance which was within the thermal noise in the system so we chose to ignore it.

At much higher velocities and especially in fluid, confined fluid layer effects between the cantilever and the sample surface will contribute substantially to the motion of the cantilever and will need to be taken into account when determining the tip-sample force. However, none of this is relevant to the problem of converting cantilever shape into cantilever force. In other words, these issues are important in determining tip-sample forces, but not important in determining cantilever shape.

Regarding non-linearity of piezo scanners, the approach was made using an Npoint stage with capacitance sensor (±0.1 nm). Any hysteresis in the motion of the piezos was taken into account by using the calibrated sensor values instead of the drive signal sent to the stage.

Influence of Ambient Humidity on the measurements

The humidity was held constant at 43±5% RH and a 20°C temperature throughout the experiment. It is likely that the onset of the snap-to-contact was initiated due to thermally driven oscillations in the fluid layers on the tip and/or mica surface. The retraction of the cantilever was not the focus of the experiment therefore the formation and snapping of any meniscus was not explored. It would be expected that as the humidity increased, the size and strength of any meniscus force would increase, though this is not taken into account in the model used. Overall, these issues are of central importance in the study of the origins of tip/sample forces probed using F(s) curves but not in characterizing the kinematics of the cantilever motion. For our purposes, as long as some force, be it capillary, vDW, or electrostatic, was present that initiated a snap-to-contact, then the lever is made to move in a non-equilibrium manner as the tip snaps down to the surface.

EXPERIMENTAL RESULTS

Position vs. time traces were collected as explained in the previous section. Figure 2 labels the 210 positions at which time trace data were taken. We were particularly careful to gather information from bending deflections only. It is known that cantilevers tend to exhibit torsion upon snap-to-contact. The exact lateral location of the tip on the Bruker MSNL B cantilever used is not always centered on the cantilever. Therefore, the cantilever can experience a moment about the tip when the tip experiences a force such as a snap-to-contact event. The cantilever displacement was measured at points taken along a line that intersected the tip. In doing so, the

effect of the torsional modes are minimized in the data. Data previously collected by Payton et al.[1,2] using a similar method have been shown to be modelled well by a bending mode only FEA model[3] indicating that, with the correct placement of the points at which data is collected, the torsional modes can be ignored.

An example of a time trace for a single snap at a single location on the lever is shown in Figure 3. To ensure that the input to our model matched the initial conditions of the theory we used, it was necessary to have no displacement at early times corresponding to a motionless cantilever when the tip and sample are well separated and not interacting. To achieve this, we found the average displacement value prior to the snap, and then used the collected data to find the last time the recorded data achieved this value prior to entering the snap-in region. We then appended ten identical values of this average to the start of each snap thus guaranteeing a well-behaved input.

At some point, the tip-sample interaction becomes non-negligible and a downward trend corresponding to an attraction occurs. This is seen in Figure 3 starting at around $5\,\mu s$. Eventually, the tip feels the repulsive force due to a combination of a confined fluid layer and Pauli exclusion acting on electrons in the tip and the surface. This slows the cantilever and eventually causes it to reverse direction.

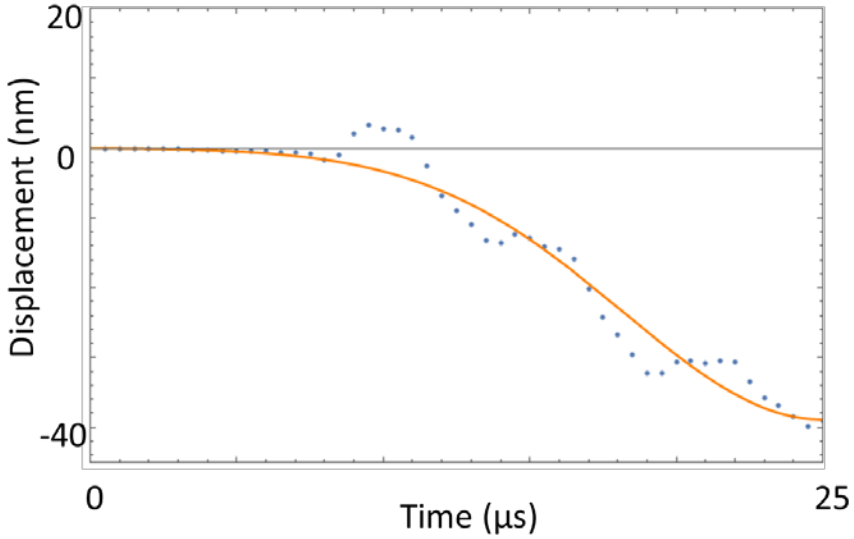

Figure 3. Snap-to-contact displacement of a point ~15 µm from the free end of the cantilever as a function of time. Also shown is a best fit EVE curve[29] that helps the eye follow the general trend and is useful in matching the phases of multiple data sets like the one shown.

Apparent in the typical snap-to-contact event shown in Fig. 3, are a few plateaus in the traverse of the cantilever toward the surface. In some cases, the path of the lever even seems to reverse direction for a short time before continuing on down. It is possible that high frequency oscillations of the cantilever due to the thermal bath or some other source existed as the state of the lever prior to its entering the snap-to-contact regime. It is also possible that the short time events came from some electronic source related to the Doppler system used to measure the cantilever displacements. Conventional cantilever analysis would treat these as higher order normal modes. However, the amplitude, frequency, and phase of such modes all depend intimately on the boundary conditions at the hanging end of the cantilever. During snap-to-contact, this boundary is changing so rapidly that the lever is unable to move through a complete period of an oscillation before the boundary condition has substantially changed because the tip is now closer to the surface. Thus, the concept of a mode is not well defined during the snap-to-contact event. In an attempt to determine what range of frequencies the cantilever used would go

through as it traversed the snap-to-contact, we solved the equations 4 and 5 in reference [33]. In going from large separation to contact: the first free mode of the lever goes from 15 kHz to 0 kHz, the second free mode goes from 95 kHz to 75 kHz, and the third free mode goes from 266 kHz to 253 Hz. None of these ranges includes the observed oscillation frequency near 200 kHz seen in our data. This makes it unlikely that these oscillations are a reflection of higher order

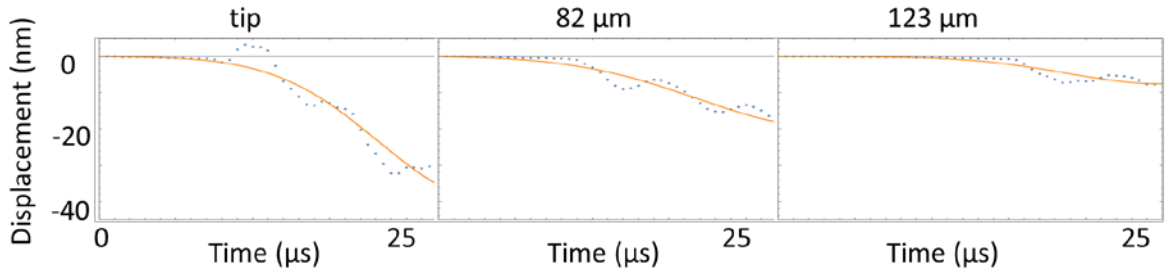

Figure 4. Displacement vs. time curves for three locations along the lever: at the tip, 82 um back from the tip, and 123 um back from the tip.

resonances in the lever. As an initial attempt at analyzing this complex data, we decided to focus on the main feature of the monotonic descent of the lever toward the surface. To extract this feature from the data, we found best-fit EVE curves[32, 35] and used these functions as inputs to our theoretical analysis.

Figure 4 shows three displacement vs time curves corresponding to three different locations along the cantilever. As one looks further away from the tip, the onset of the snap-in gets later in time and the amplitude of the displacement decreases. The general trend is clearly downward, however there are a few steps in the recorded path along the way as described in Figure 3 above. The EVE fits are shown as the solid lines in each of the plots. In general, the EVE function fit the data very well.

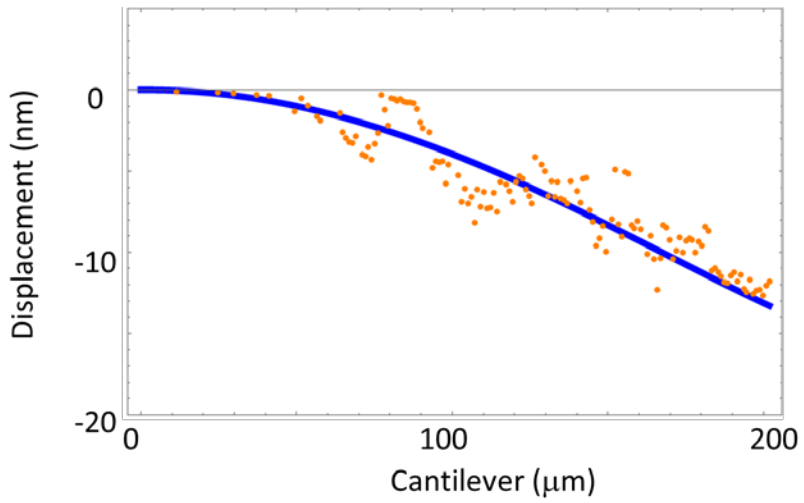

Figure 5. Instantaneous positions of monitored points along the cantilever are shown 15 µsec after the start of the snap-to-contact. The trend line represents the cantilever.

A useful alternative view of the cantilever motion is given in Figure 5. There, a snapshot of the full cantilever shape is created by plotting the position of each individual point along the lever at one instant in time.

COMPARISON BETWEEN THEORY AND EXPERIMENT

Since the Euler-Bernoulli differential equation is 4^{th} order in space and 2^{nd} order in time, six constraints are needed to solve it. The constraints are obtained by setting two initial conditions and four boundary conditions. Our solution uses two initial conditions in the form of the shape of the cantilever at two consecutive early times. It is assumed that the force on the cantilever is small enough at these early times to allow for quasi-static motion. Thus, the two initial shapes are taken from unequivocally known static shapes under an external force at the free end. This effectively provides the initial shape of the cantilever and its initial state of velocities. In addition, we use two boundary conditions at the attached point namely, that the cantilever is fixed there and that it does not bend. The last two conditions are obtained by setting the vertical displacement and the slope at the hanging end of the cantilever equal to their experimentally measured values. With that input, we numerically solve the Euler-Bernoulli equation and predict the motion of all the cantilever points from the free to the fixed end. This theoretical cantilever shape vs time, relying only on measurements made near the free end of the cantilever, is then compared to the full experimentally measured motion along the whole cantilever.

To implement the solution, we took a few of the position-vs-time curves near the end of the lever and used them to determine the slope at the end of the lever. This allowed us to mimic the information available in most commercial atomic force microscopes using the direct displacement measurements provided by our Doppler technique. We emphasize that only data near the end of the lever was used to compute the entire shape of the lever. These computed shapes were then compared against the Doppler vibrometry experiments. We did this comparison in two ways. First, we looked at the displacement vs time curves for individual

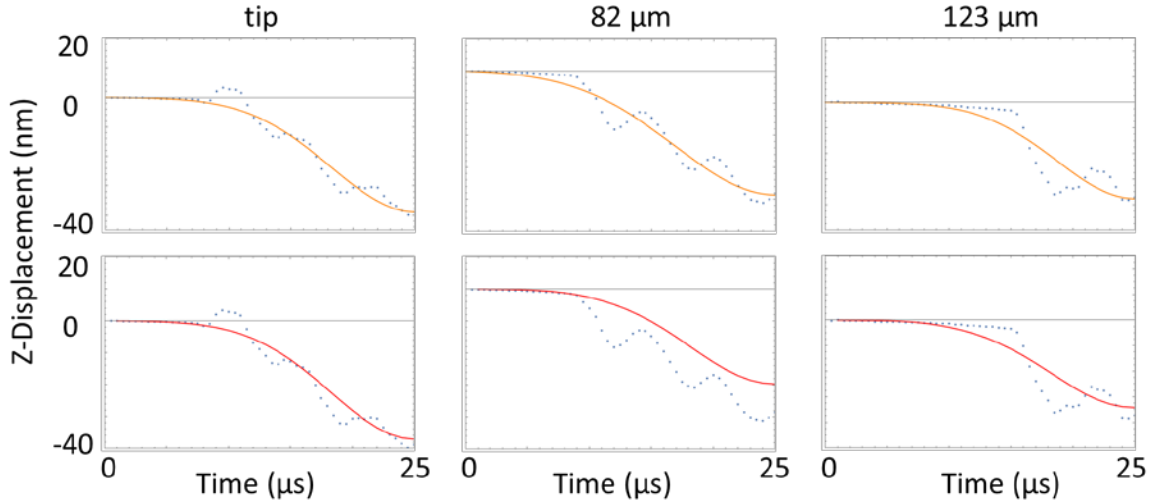

Figure 6. Comparison of experiment with theory at individual points along the long axis of the cantilever: tip(left columns), 82 um back from tip (middle columns), 123 um back from tip (right columns). The top row shows experimental displacement vs. time curves (blue dots) along with the best fit EVE function (solid yellow line) to each curve. The bottom row shows the same experimental data but the solid red lines are the theoretical outputs from numerical solution to the Euler Bernoulli equation as described in the text.

locations along the lever. Second, we looked at the entire shape of the lever at a given time point.

To compare theory with experiment at single points along the lever, Figure 6 shows time traces at the same three points as in Figure 4 together with the theoretical outputs. The top row of curves shows these experimentally determined plots with the EVE function best fits. The lower set of curves shows the same experimental data but the solid lines represent the output from the model which used the Euler-Bernoulli solutions using data only near the end of the lever to compute the solid curves. Experiment and theory agree well at the tip (left most plots in Fig. 7) which is expected since this is what was used as the input to the model. Experiment and theory also fit well 123 μm back from the end of the lever. However, the fit 82 μm back from the end is not as good. Looking carefully at noise in the system will allow us to determine if the overall motion of the cantilever is well captured by our model or not.

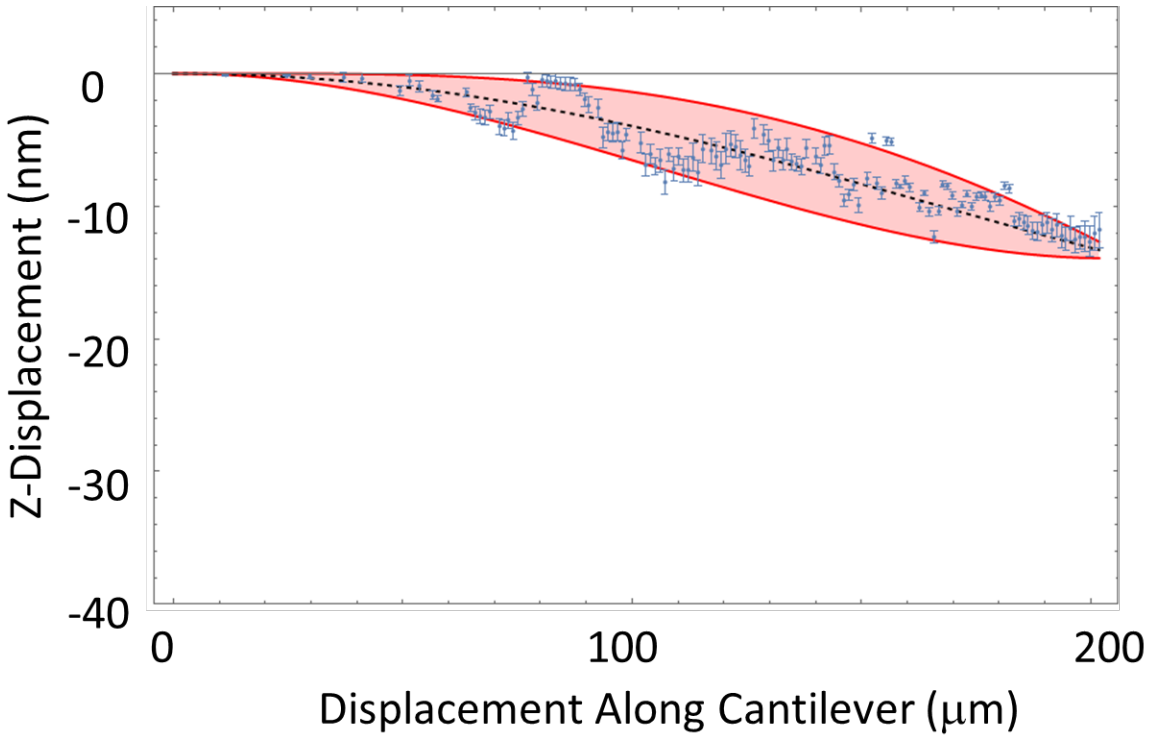

Figure 7. Snapshot of the shape of the full cantilever at an instant in time. Blue dots are the experimentally measured points. The black dotted line is the best fit to the theory. The red shaded region corresponds to the range of theoretical curves obtained using +/- one standard deviation in the experimental input error to the measured slope at the end of the cantilever.

Substantial measurement noise propagated from the input of our model to its output. To understand how this affected the deviation between experiment and theory, it was necessary to perform an error analysis that contained as much of the noise and its propagation through the model as possible. To this end, we used five data points near the end of the cantilever to determine its slope. In the absence of noise, any pair of these five points would have yielded the same slope. Because of the presence of noise, we obtained a population of slopes from all pair combinations and used this to compute a standard deviation of the noise. This population was used in the analysis that follows to find an envelope of model shapes of the cantilever.

As a second way to compare experiment with theory, a typical snapshot of the lever with errors displayed is shown in Figure 7. The blue points with small error bars represent the experimentally determined locations of the lever at that particular location along the long axis of the lever. The dashed black line corresponds to the average theoretical value for the z -position of each location along the long axis of the lever. The shaded region represents the error in the model output based on the measured error in the input data. Specifically, five locations near the end of the lever were used. These locations were close enough together so that they should have all produced the same slope. In fact, they provided a range of slopes. The standard deviation of the slope was found and then the mean plus or minus one standard deviation was used as an input to the model. This produced a range of shapes that falls within the shaded region. Note: this slope is used as an input at each time point in the model. Thus, a different standard deviation and a different shaded region were computed at each time point.

Figure 8 shows six different snapshots of the snap-to-contact portion of the curve displayed in the same way as Figure 7. A movie showing the whole trajectory of the whole cantilever during the snap-to-contact corroborates what is displayed in Figure 8 (see supplemental data). While there are some experimental points that fall outside the shaded region, it is clear that the majority of experimental points fall within the computed error. For the six typical snapshots shown in Figure 9, an average of 71% of the experimental points fall within one standard deviation of the mean. Assuming a Gaussian distribution of the experimental points about some "true mean," the obtained distribution of experimental points about the theoretical curves is as expected.

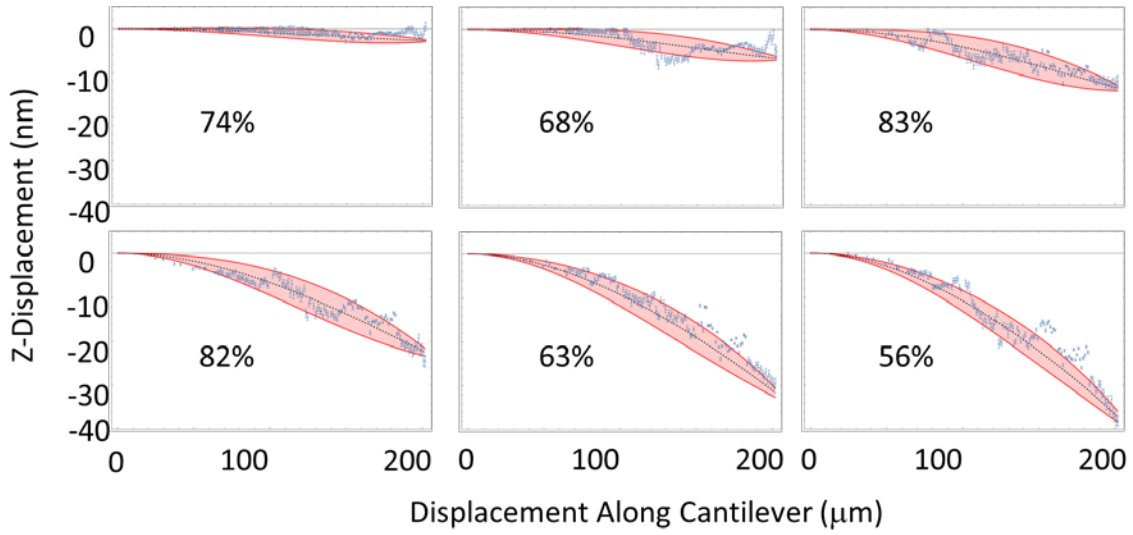

Figure 8. Superimposed experimental measurements and theoretical predictions based on the Euler-Bernoulli equation. Experimental results are shown as dots. Theory is displayed as a dashed line representing the best fit cantilever shape with a shaded region around it representing theoretical outcomes that fall within one standard deviation of the experimental means assuming normally distributed errors. Percentages reflect how many of the experimental points fall within the shaded regions around the theoretical curves.

This gives substantial evidence that the Euler-Bernoulli equation in general, and our model for solving the ill-posed problem present when trying to convert the data provided by

most commercial atomic force microscopes into known cantilever shapes, provide correct solutions.

CONCLUSIONS

We find that the Euler-Bernoulli theory is an appropriate framework to predict the kinematics of the cantilever during the far-from-equilibrium snap-to-contact event. We show by direct comparison with Doppler vibrometry experiments the validity of the force-separation reconstruction algorithm based on the Euler-Bernoulli equation. Specifically, we did this comparison for the case of a cantilever undergoing far-from-equilibrium motion driven by non-linear forces during the snap-to-contact event. The relevance of our result is that, unlike in the experiment used here, conventional atomic force microscopy experimental conditions allow collection of the slope or position vs time at only a single point on the cantilever. While our rendering of the Euler-Bernoulli-based algorithm allows for the reconstruction of the full shape of the cantilever at all times, the reliability of these shapes rests ultimately on the validity of the model used. Our proof thus paves the way to use our reconstruction algorithm under conventional atomic force microscopy operating conditions. The time-consuming multiple Doppler vibrometry measurement, while central to our test, is shown here to be no longer needed when running conventional atomic force microscopy experiments Indeed, once one knows that Euler Bernoulli can be used during snap-to-contact to predict the shape of the cantilever, the bending forces are readily attainable. In other words, our results should extend the ability to produce accurate force-separation curves from conventional voltage-time traces into far-from-equilibrium motion and non-linear interactions.

ACKNOWLEDGMENTS

This project is funded by the National Science Foundation Grant No. CHE-1508085, The Alexander Fund, and The Kressel Fellowship (DF).

REFERENCES

1. ZYPMAN F. Fast Atomic Force Microscopy. Encyclopedia of Nanoscience and Nanotechnology 2004. p. 307.
2. Eppell SJ, Liu YH, Zypman FR. Accuracy of AFM force distance curves via direct solution of the Euler-Bernoulli equation. AIP Advances. 2016;6(3).
3. Todd BA, Eppell SJ, Zypman FR. Squeezing out hidden force information from scanning force microscopes. Applied Physics Letters. 2001;79(12):1888-90.
4. Zhang JB, Xi N, Li GY, Su CM, Ieee. Atomic Force Microscopy sensing using multiple modes2006. 3928-+ p.
5. Dufrene YF, Ando T, Garcia R, Alsteens D, Martinez-Martin D, Engel A, et al. Imaging modes of atomic force microscopy for application in molecular and cell biology. Nature Nanotechnology. 2017;12(4):295-307.
6. Santos S, Lai CY, Olukan T, Chiesa M. Multifrequency AFM: from origins to convergence. Nanoscale. 2017;9(16):5038-43.
7. Xu K, Sun WH, Shao YJ, Wei FN, Zhang XX, Wang W, et al. Recent development of PeakForce Tapping mode atomic force microscopy and its applications on nanoscience. Nanotechnol Rev. 2018;7(6):605-21.
8. Voigtländer B. Scanning probe microscopy. Berlin: Spring; 2015.
9. Chen L, Wen JL, Zhang P, Yu BJ, Chen C, Ma TB, et al. Nanomanufacturing of silicon surface with a single atomic layer precision via mechanochemical reactions. Nature Communications. 2018;9.
10. de Pablo PJ. Atomic force microscopy of virus shells. Seminars in Cell & Developmental Biology. 2018;73:199-208.
11. Gao Y, Wang JK, Zhong J, Wang YL, Yin QX, Hou BH, et al. Application of Atomic Force Microscopy in Understanding Crystallization Process. Science of Advanced Materials. 2017;9(1):89-101.
12. Hussain D, Ahmad K, Song JM, Xie H. Advances in the atomic force microscopy for critical dimension metrology. Measurement Science and Technology. 2017;28(1).
13. Li M, Dang D, Xi N, Wang YC, Liu LQ. Nanoscale imaging and force probing of biomolecular systems using atomic force microscopy: from single molecules to living cells. Nanoscale. 2017;9(45):17643-66.
14. Li M, Xi N, Wang YC, Liu LQ. Applications of Multiparametric Imaging Atomic Force Microscopy in Probing Cellular and Molecular Mechanics. Progress in Biochemistry and Biophysics. 2018;45(11):1106-14.
15. Ruggeri FS, Sneideris T, Vendruscolo M, Knowles TPJ. Atomic force microscopy for single molecule characterisation of protein aggregation. Archives of Biochemistry and Biophysics. 2019;664:134-48.
16. Setvin M, Wagner M, Schmid M, Parkinson GS, Diebold U. Surface point defects on bulk oxides: atomically-resolved scanning probe microscopy. Chemical Society Reviews. 2017;46(7):1772-84.
17. Sharma S, LeClaire M, Gimzewski JK. Ascent of atomic force microscopy as a nanoanalytical tool for exosomes and other extracellular vesicles. Nanotechnology. 2018;29(13).
18. Zhong J, Yan J. Seeing is believing: atomic force microscopy imaging for nanomaterial research. Rsc Advances. 2016;6(2):1103-21.

19. Pavlicek N, Gross L. Generation, manipulation and characterization of molecules by atomic force microscopy. Nature Reviews Chemistry. 2017;1(1).
20. Todd BA, Eppell SJ, Zypman FR. Improved analysis of the time domain response of scanning force microscope cantilevers. Journal of Applied Physics. 2000;88(12):7321-7.
21. Schroeter K, Petzold A, Henze T, Thurn-Albrecht T. Quantitative Analysis of Scanning Force Microscopy Data Using Harmonic Models. Macromolecules. 2009;42(4):1114-24.
22. Payam AF, Fathipour M. Modeling And Dynamic Analysis Of Atomic Force Microscope Based On Euler-Bernoulli Beam Theory. Digest Journal of Nanomaterials and Biostructures. 2009;4(3):565-78.
23. Gates RS, Pratt JR. Accurate and precise calibration of AFM cantilever spring constants using laser Doppler vibrometry. Nanotechnology. 2012;23(37).
24. Payton OD, Picco L, Miles MJ, Homer ME, Champneys AR. Modelling oscillatory flexure modes of an atomic force microscope cantilever in contact mode whilst imaging at high speed. Nanotechnology. 2012;23(26).
25. Zhou XL, Fu J, Li FX. Contact resonance force microscopy for nanomechanical characterization: Accuracy and sensitivity. Journal of Applied Physics. 2013;114(6).
26. Laurent J, Steinberger A, Bellon L. Functionalized AFM probes for force spectroscopy: eigenmode shapes and stiffness calibration through thermal noise measurements. Nanotechnology. 2013;24(22).
27. Payam AF. Sensitivity of flexural vibration mode of the rectangular atomic force microscope micro cantilevers in liquid to the surface stiffness variations. Ultramicroscopy. 2013;135:84-8.
28. Villanueva LG, Karabalin RB, Matheny MH, Chi D, Sader JE, Roukes ML. Nonlinearity in nanomechanical cantilevers. Physical Review B. 2013;87(2).
29. Zhou XL, Wen PF, Li FX. Vibration analysis of atomic force microscope cantilevers in contact resonance force microscopy using Timoshenko beam model. Acta Mechanica Solida Sinica. 2017;30(5):520-30.
30. Wagner R, Killgore J. Reconstructing the distributed force on an atomic force microscope cantilever. Nanotechnology. 2017;28(10).
31. Todd BA, Eppell SJ. Probing the limits of the Derjaguin approximation with scanning force microscopy. Langmuir. 2004;20(12):4892-7.
32. Mehlman J, Zypman FR. Scanning Probe Microscope Force Reconstruction Algorithm via Time-Domain Analysis of Cantilever Bending Motion. Journal of Advanced Microscopy Research. 2014;9(3):268-74.
33. Zypman FR, Eppell SJ. Analysis of scanning force microscope force-distance data beyond the Hookian approximation. Journal of Vacuum Science & Technology B. 1998;16(4):2099-101.
34. Payton OD, Picco L, Champneys AR, Homer ME, Miles MJ, Raman A. Experimental observation of contact mode cantilever dynamics with nanosecond resolution. Review of Scientific Instruments. 2011;82(4):5.
35. Eppell SJ, Feinstein M, Li L, White B, Zypman FR. Signal distortion in atomic force microscopy photodetector. Review of Scientific Instruments. 2017;88(10).